Microwave spectra of *d*-wave superconductors

C. T. Rieck and K. Scharnberg
Abteilung für Theoretische Festkörperphysik, Universität Hamburg, Jungiusstrasse 11, D-20355 Hamburg, Germany

J. Ruvalds
Department of Physics, University of Virginia, Charlottesville, Virginia 22903
(Received 4 December 1998; revised manuscript received 20 May 1999)

A theory of the anomalous microwave conductivity and surface resistance of high-temperature superconductors is developed for a nested Fermi surface. The damping Γ is derived for electron collisions across nearly parallel orbit segments. Above the superconducting temperature $\Gamma(\omega,T)$ is linear in frequency ω and temperature T, in accord with the anomalous non-Drude conductivity which differentiates high-T_c cuprates from conventional metals. In the superconducting state a *d*-wave energy gap suppresses the damping—by reducing available scattering states—and thus explains why the YBCO microwave surface resistance R_s drops so dramatically when the temperature is a few degrees below $T_c = 90$ K. Numerical calculations of the infrared conductivity, reflectivity, microwave R_s, and penetration depth are presented, and comply with the YBCO experimental data if the gap has a large maximum value $\Delta_{dm} \simeq 4T_c$. The cuprate spectral shapes differ notably from conventional BCS theory. [S0163-1829(99)02338-3]

I. INTRODUCTION

When certain copper oxide metals become superconducting, their microwave surface resistance R_s drops by four orders of magnitude within a few degrees of the transition temperature $T_c \simeq 90$ K. This remarkably small R_s reduces energy loss and benefits microwave sensor and communications technology, while the stability of R_s at low T provides another bonus. In addition, the frequency variation of the conductivity provides intriguing clues to the physical nature of the charge carriers and exposes the symmetry of the superconducting state.

The objective of the present work is to develop a theory of the microwave spectra for a superconductor with a *d*-wave energy gap, using a physical basis that produces the anomalous quasiparticle damping which is a key feature[1] of cuprates at higher temperatures. Electron collisions on a nested Fermi surface yield a damping that is linear in frequency and temperature, and a microscopic theory[2] demonstrates that these phenomena explain cuprate conductivity anomalies if the Coulomb repulsion U is of intermediate strength. Here we extend this nested Fermi-liquid (NFL) theory to a superconducting state that is characterized by a *d*-wave energy gap.

Our analysis was motivated by the Hardy group[3] discovery of a sharp suppression of the quasiparticle damping in the superconducting state of YBCO, which is much steeper than expected from standard BCS theory. As seen in Fig. 1, their microwave surface resistance R_s data show an amazing drop in surface resistance R_s by four orders of magnitude as the temperature is lowered two degrees below $T_c = 92$ K.

The classic BCS theory, which considers electron-phonon damping, yields the solid R_s curve[4] that is far above the YBCO data in Fig. 1. The BCS theory fits R_s data for ordinary superconductors, like lead and niobium, quite well with an isotropic energy gap, and the electron-phonon interaction is believed to be the dominant coupling source in simple metals. Phonon mediated *s*-wave pairing in standard superconductors is also well established. From a phonon perspective it is remarkable that a combination of impurity scattering and the Gruneisen form of electron-phonon damping can reproduce some of the R_s features in Fig. 1.[5] However, the classic Holstein theory shows that the conductivity becomes independent of frequency above the Debye cutoff for phonons,[6] and this feature contradicts the cuprate data.

Various experiments on cuprates suggest an alternate

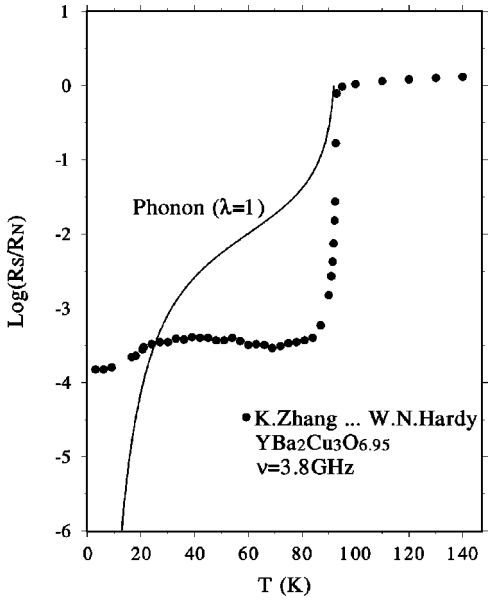

FIG. 1. The microwave surface resistance data points of Ref. 3 show the sharp drop in $R_s(T)$ within the YBCO superconducting state, that occurs a few degrees below $T_c = 92$ K. By contrast the standard BCS model with an isotropic *s*-wave energy gap, a Debye energy $\Theta_D = 104$ meV, and an electron-phonon coupling $\lambda = 1$ yields the solid curve which remains far above the data in the temperature range 20 K$< T < T_c$.

source of damping, and the compelling evidence for a *d*-wave energy gap requires a novel pairing mechanism for their high-T_c superconductivity. In particular, infrared reflectivity experiments on optimally doped cuprates discovered that the electron damping is linear in frequency ω up to the 1-eV range.[1] Also, dc resistivity measurements reveal that the damping becomes proportional to T in the static $\omega=0$ limit. All high-T_c alloys exhibit these damping mysteries, whereas oxygen doping transforms the resistivity of cuprate alloys to a T^2 form—and simultaneously lowers T_c.

Fermi-liquid (FL) damping is quadratic in ω and T, because the Pauli exclusion principle limits available electron collision[1] states. The usual assumption of a spherical Fermi surface yields a weak FL damping which is proportional to the small ratio $(T/E_F)^2$ where E_F is the Fermi energy.

Damping with a linear T and ω variation has been derived for electrons colliding on nested Fermi-surface segments: These trajectories have a phase space that is analogous to a system of reduced dimensionality. If scattering with a momentum transfer equal to the nesting vector $\mathbf{Q}$ is dominant, a microscopic theory yields a quasiparticle damping $\Gamma_{NFL} \approx [U/W]^2\omega$ in the zero-temperature limit.[2] This nested Fermi-liquid (NFL) theory computes self-energy and vertex corrections[1] to the conductivity, and fits the anomalous infrared data on cuprates if the Coulomb coupling U is comparable to the bandwidth W. Similarly the linear T dependence of the NFL damping can be attributed to nesting.

The NFL damping originates from an intriguing scaling of the spin susceptibility as a function of ω/T. The scaling can be easily derived for noninteracting electrons whose energy dispersion satisfies the nesting condition $\epsilon_{\mathbf{k}+\mathbf{Q}} \cong -\epsilon_{\mathbf{k}}$. By comparison, the susceptibility of a free-electron gas is nearly independent of temperature. Neutron-scattering experiments confirm the NFL scaling[1] in large cuprate crystals.

In order to derive the NFL collision damping in a superconducting state appropriate to cuprates, we derive analytic formulas for the spin susceptibility which includes an energy gap with *d*-wave symmetry. Then we compute the damping numerically as a function of frequency and temperature. Finally we compute the microwave conductivity, infrared reflectivity, surface resistance, and penetration depth.

Previous relevant studies include the microwave conductivity peak (just below T_c) which was discovered and interpreted in terms of a damping reduction by Nuss *et al.*[7] The phenomenological ''marginal'' Fermi-liquid[8] polarizability yields a conductivity peak when energy gaps are used to cut off their model susceptibility at low energy.

Our previous microwave analysis[9] used an isotropic *s*-state energy gap, which accounts for a drop in the surface resistance near T_c but contradicts the low-temperature microwave spectra. A thorough investigation of electromagnetic properties of high T_c films has been performed within the NFL formalism by Scharnberg's group.[10] They focus on the temperature variation of the microwave response, whereas the present work emphasizes the frequency dependence.

Anderson *et al.*[11] have proposed a theory of the linear ω damping using self-energy insertions for a Luttinger liquid. Traditional conductivity calculations for a Luttinger liquid give a gaplike structure at low frequencies,[12] which is caused by separation of spin and charge degrees of freedom in a one-dimensional model.

Tight-binding energy bands have been used to compute the influence of energy gaps on microwave response by various groups.[13–15] Phenomenological forms[16,17] for the susceptibility also produce conductivity peaks. Impurity scattering has been analyzed for superconductors with various energy gap symmetries. Quinlan *et al.*[18] examined the influence of a *d*-wave energy gap and impurity scattering on the frequency variation of the conductivity, although they do not consider nesting in their tight-binding band model.

Experimental evidence for a *d*-wave energy gap in high-temperature superconductors includes the elegant quantum interference mesurements which reveal a sign change in the order parameter,[19] photoemission probes of the gap asymmetry, NMR spectra, Raman line shapes, and tunneling measurements. The latter three probes detect a *d*-wave superconducting density of states with a surprisingly large energy gap $\Delta_m \cong 6T_c$,[1] and we find here that a strong coupling value is also needed to fit electromagnetic response features of the YBCO superconducting state.

Electron-doped cuprates differ from the high-T_c materials by having a Fermi-liquid type of damping, lower $T_c \approx 20$ K, and a rounded Fermi surface (discerned by photoemission experiments in NCCO).[20] The NCCO surface resistance spectra and penetration depth are fitted accurately by ordinary BCS electrodynamics with an isotropic weak-coupling energy gap.[21] Hence these electron-doped materials are outside the scope of the present analysis.

The correlation of high-T_c values with anomalous damping in cuprates may indicate that nesting provides a theoretical link to *d*-wave pairing. The present examination provides further impetus to the challenge of the *d*-wave mechanism by elucidating the strong-coupling nature of the scattering and the energy gap.

A spin-fluctuation exchange theory for *d*-wave pairing was originally examined by Berk and Schrieffer,[22] and independently by Kohn and Luttinger,[24] but unforunately their estimates for a spherical Fermi surface yield negligible T_c. Nonetheless, this concept was revived in connection with heavy-fermion metals and the anisotropic copper oxide planar structures. Scalapino's group,[25] and others, find that the RPA susceptibility series can raise T_c for a tight-binding energy band in the vicinity of a spin-density-wave (SDW) instability.[23] Schrieffer[26] has argued that vertex corrections are mandated near the SDW transition, and conserving methods have been developed by Bickers[27] and others to cope with higher-order self-energy and vertex corrections for a Hubbard model.

Recent calculations for a nesting model shows how vertex corrections create a many-body effect[28] that appears as a singularity in the spin susceptibility at low T and ω. The nonuniversal power-law exponents for the divergent susceptibility are in line with the neutron-scattering data which discovered this anomalous susceptibility response at a nesting vector in the LSCO cuprate.[29]

Nesting can enhance the spin-exchange mechanism[1] by optimizing the overlap of *d*-wave orbitals in the case of selected topologies that resemble a nearly square Fermi surface. Thus, using a tight-binding band suited to the Fermi surface of the Bi2212 superconductor, *leading-order* calculations[30] yield $T_c = 85$ K for a Hubbard interaction U that is comparable to the bandwidth. If the nesting vector

moves closer to the ideal value at half filling, the spin-density wave instability[23] overcomes *d*-wave superconductivity—within the random-phase approximation (RPA). In the opposite limit, a small nesting vector yields a neglibible supercondcuting T_c. Photoemission spectra[31] reveal that the Bi2212 Fermi surface is nested in the form of a square with rounded corners, and show a smaller nesting vector in Bi2201 which is compatible with its lower T_c.

We derive the spin susceptibility and damping in Sec. II. The formalism for the electrodynamic response is developed in Sec. III, and then applied to microwave surface resistance, conductivity, reflectivity, and the penetration depth in Sec. IV. Conclusions of our analysis are presented in Sec. V.

II. NESTED ELECTRON COLLISIONS

A. Susceptibility and damping for $T>T_c$

Electron (or hole) interactions are represented by the Hubbard Hamiltonian

$$H=\sum_{k\cdot\sigma}\epsilon_k c^{+}_{k\sigma}c_{k\sigma}+U\sum_i n_{i\uparrow}n_{i\downarrow}, \tag{1}$$

where U is the onsite Coulomb repulsion, $c_{k\sigma}$ is the destruction operator for an electron with momentum k and spin σ, and $n_{i\sigma}$ designates the occupation of an electron at site i. This choice of interaction emphasizes the role of the spin susceptibility χ in the scattering cross section, although the generalization to the charge channel is straightforward.

The quasiparticle damping for a nested Fermi surface (in the Born approximation) can be expressed as

$$\Gamma_{NFL}(\omega,T)=\frac{1}{2}N(0)U^2\int d\omega' \times\left[\coth\left(\frac{\omega'}{2T}\right)-\tanh\left(\frac{\omega'-\omega}{2T}\right)\right]\chi''_{NFL}(\omega',T), \tag{2}$$

where $N(0)$ is the density of states at the Fermi energy. The spin susceptibility within the nesting approximation $\epsilon_{k+Q}\cong-\epsilon_k$ takes the unconventional form[2]

$$\chi''_{NFL}(\omega,T)=\frac{\pi N_o}{2}\tanh\left(\frac{\omega}{4T}\right). \tag{3}$$

The scaling of the NFL susceptibility as a function of ω/T generates the anomalous linear T damping in the static limit $\omega=0$, which follows by inspection of Eq. (2). In the zero-temperature limit, the thermal factors reduce to step functions, and then the integration in Eq. (2) gives a linear ω variation of the damping. The collision damping becomes[2] $\Gamma_{NFL}\cong(\pi/2)U^2N(0)^2\max[1.23T,|\omega|]$, and its magnitude is in line with cuprate conductivity data if the Coulomb coupling satisfies $UN(0)\sim1$. Quantitative accuracy requires terms beyond the Born approximation, such as the self-consistent inclusion of self-energy and vertex corrections to the susceptibiltiy which are beyond the scope of the present analysis.

The scaling of the susceptibility in ω/T distinguishes the nesting approach from the conventional Fermi-liquid (FL) theory, where χ''_{FL} is only weakly temperature dependent. Scaling of the actual susceptibility was observed in $YBa_2Cu_3O_{6.5}$,[32] and by neutron-scattering experiments on LSCO compounds as well.[1] Scaling is easy to derive for a nested Fermi surface without any interactions, and a formal proof[33] of scaling preservation by self-energy corrections and vertex corrections has recently been derived.

B. Superconducting state

We generalize the NFL formalism to include a superconducting energy gap which depletes the electron density of states $N(\omega)$ and also modifies the susceptibility. This leads to a quasiparticle damping in the superconducting state

$$\Gamma_{NFL}(\omega,T<T_c)=\frac{U^2}{2}\int d\omega' \times\left[\coth\left(\frac{\omega'}{2T}\right)-\tanh\left(\frac{\omega'-\omega}{2T}\right)\right] \times N(|\omega-\omega'|)\chi''_{NFL}(\omega',T<T_c). \tag{4}$$

The imaginary part of the NFL susceptibility χ''_{NFL} in the superconducting state depends on the energy gap and the coherence factors which distinguish the charge channel from the spin susceptibility. The general form of the spin susceptibility becomes

$$\chi(q,\omega)=\sum_{k,l,m}\frac{lA(l,m)}{N}\frac{\tanh(E_k/2T)-ml\tanh(E_{k+q}/2T)}{\omega+lE_k+mE_{k+q}+i\delta}, \tag{5}$$

where $l,m=\pm1$, and the coherence factor is

$$A(l,m)=\frac{1}{4}\left[1+lm\left(\frac{\epsilon_k\epsilon_{k+q}+\Delta(k)\Delta(k+q)}{E_kE_{k+q}}\right)\right] \tag{6}$$

with $E_k=+\sqrt{\epsilon_k^2+\Delta^2(k)}$.

The energy gap equation for cuprates remains unresolved, especially since spin-fluctuation mechanisms of the pairing interaction require a susceptibility whose momentum and energy dependence is model dependent. The self-energy and vertex corrections, which renormalize the pairning kernel significantly in cases with nesting, require a strong-coupling analysis which is not yet available. For example, numerical solutions of the parquet diagrams for a nesting model[34] illustrate the complexity of competing *d*-wave and SDW channels. Hence we choose a phenomenological form for the gap whose maximum amplitude is given by

$$\Delta_{dm}=aT_c\tanh[b\sqrt{T_c/T-1}]. \tag{7}$$

A standard isotropic *s*-wave gap Δ_s in the weak-coupling limit would give $a=1.76$ and $b=1.74$. A conventional *d*-wave model with an isotropic Fermi surface provides similar values.[35]

Evidence for a strong-coupling *d*-wave gap in cuprate superconductors is provided by NMR, Raman, and tunneling data. These probes suggest[1] values in the range of $a\simeq6.0$ and $b\simeq1.5$, which indicates a zero-temperature gap value $\Delta_{dm}\approx6T_c$. The present electromagnetic response analysis tends to support a strong-coupling gap as well.

For an *s*-wave superconductor, the imaginary part of the susceptibility reduces to

$$\chi''_{NFL,s}(\omega,T)=\frac{\pi N_o}{2}\frac{\sqrt{\omega^2-4\Delta_s^2}}{|\omega|}\tanh\left(\frac{\omega}{4T}\right)\Theta(\omega-2\Delta_s). \tag{8}$$

The Heaviside function Θ cuts off the susceptibilty, eliminates available electron-scattering states below $2\Delta_s$ and thus strongly reduces the NFL damping. The influence of the *s*-state gap on the electromagnetic properties was computed previously,[9] and the resulting exponential decrease of R_s at low T, which disagrees with the data in Fig. 1, motivated us to focus attention on *d*-wave gap structure.

In the cuprates, the superconducting electron dynamics are restricted to the CuO_2 planes, which suggests a two-dimensional $d_{x^2-y^2}$ order parameter:

$$\Delta_d(\vec{k})=\Delta_{dm}(T)\cos(2\phi), \tag{9}$$

where the angle ϕ is measured from the k_x axis in the plane. For a nested square surface—that is expected for a half filled tight-binding energy band in cuprates—the chosen *d*-wave gap has the symmetry $\Delta_{k+Q}\cong-\Delta_k$ when the nesting vector **Q** is parallel to the (π,π) direction. This relation simplifies our derivation of the susceptibility and damping, which physically picks out scattering across nested regions of the Fermi surface as the dominant damping source.

The imaginary part of the spin susceptibility for a $d_{x^2-y^2}$ superconductor then becomes

$$\chi''_{NFL,d}(\omega,T)=\frac{\pi}{2}N_d\left(\left|\frac{\omega}{2}\right|\right)\tanh\left(\frac{\omega}{4T}\right), \tag{10}$$

where the superconducing density of states is given by

$$N_d(\omega)=\sum_{\vec{k}}\delta(\omega-E_{\vec{k}}). \tag{11}$$

Performing the energy and ϕ-angle integrations yields

$$N_d(\omega)=\frac{2\omega}{\pi\Delta_{dm}}K_e\left(\frac{\omega}{\Delta_{dm}}\right),\quad \text{for } \omega<\Delta_{dm}$$
$$=\frac{2}{\pi}K_e\left(\frac{\Delta_{dm}}{\omega}\right),\quad \text{for } \omega>\Delta_{dm}, \tag{12}$$

where K_e denotes the complete elliptic integral of the first kind. The resulting spin susceptibility for a *d*-wave superconductor has a logarithmic singularity at $\omega=2\Delta_{dm}$ and is shown in Fig. 2. It is remarkable that the superconducting gap magnitude actually exceeds the normal state $\chi''_{NFL,d}$ in the intermediate frequency range: Neutron-scattering data[36] on the LSCO superconductor demonstrates this surprising susceptibility enhancement at the nesting vector for some frequencies. Apparently the band anisotropy does not eliminate the peak structure in the density of states which arises from the *d*-wave gap. However, since $N_d(\omega)\approx\omega$ for small frequencies, and the susceptibility for a *d*-wave state is proportional to ω^2 for $\omega\ll T$, the low-frequency susceptibility is reduced by the gap formation.

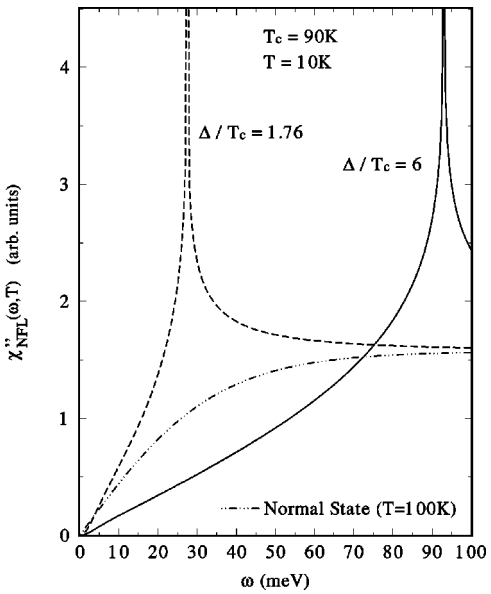

FIG. 2. Imaginary part of the NFL spin susceptibility at the nesting vector **Q** is shown as a function of frequency. The normal state (dot-dash curve) at 100 K exhibits scaling as a function of ω/T. A weak-coupling *d*-wave energy gap produces the dashed curve with a logarithmic singularity at $2\Delta_{dm}$ and enhances the susceptibility in the intermediate frequency range. The solid curve shows the significant reduction in the susceptibility for the strong-coupling gap choice $\Delta_{dm}=6T_c$.

When the gap ratio is increased to the strong-coupling value $\Delta_{dm}=6T_c$, the depleted susceptibility for $\omega<70$ meV is illustrated by the solid curve in Fig. 2. This type of reduced χ is also found by neutron-scattering experiments.[37] The susceptibility structure is the key factor in reducing available scattering states for electron collisions.

The temperature and frequency variation of the NFL susceptibility in Eq. (10) distinguishes nesting features from tight-binding model calculations away from half filling. For example, when $T>T_c$, the bare susceptibility computed by Quinlan *et al.*[18] is almost independent of T and is roughly linear in frequency. A RPA renormalization of the susceptibility will certainly change the ω variation significantly and may magnify the T dependence if the Coulomb coupling U is chosen to represent a sysetm close to a SDW instability.

The quasiparticle damping rate is obtained from Eqs. (4) and (10)–(12) by performing one numerical integration over frequency. The resulting damping is shown in Fig. 3 as a function of temperature for a low microwave frequency ($\omega=3.8$ GHz) and a coupling value $g=UN_0=1.7$. The dashed curve demonstrates that a weak-coupling *d*-wave state overestimates the damping and thus contradicts the surface resistance data of Bonn *et al.*[3] However, the strong-coupling version of the *d*-wave gap $\Delta_m=6T_c$ yields a good fit to the damping points which Bonn *et al.* surmised from their data using a semiempirical estimate.

The computed NFL damping is shown as a function of ω in Fig. 4, where the ''normal'' state (at 100 K) dashed curve is linear in frequency for $\omega\gg T$. At a temperature of 30 K the energy gap is near its maximum for this hypothetical $T_c=90$ K superconductor, and the weak-coupling gap produces the dashed damping curve which falls below the normal state damping only at low frequencies. The strong-coupling gap

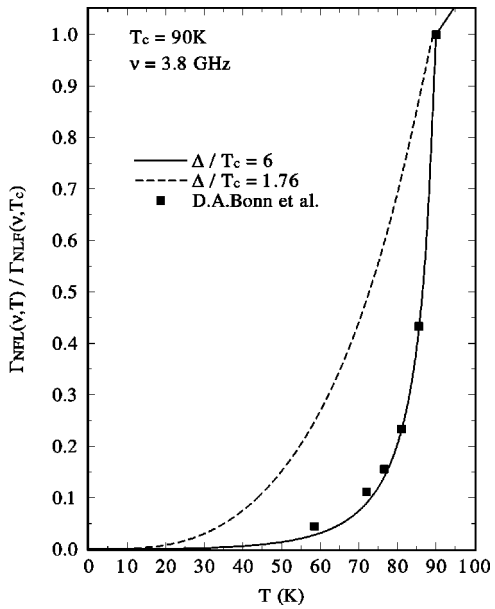

FIG. 3. Damping from electron collisions in a *d*-wave superconductor with a nested Fermi surface is shown as a function of temperature for a microwave frequency $\nu=3.8$ GHz . The dashed curve is calculated for a weak-coupling gap. The solid curve for a strong-coupling gap $\Delta_{dm}=6T_c$ yields a steeper drop in the damping by reducing available scattering states for the target as well as the incident electron. The empirical estimates from microwave surface data are the square points from Ref. 3.

ratio $\Delta_{dm}=6T_c$ yields the solid curve with a significantly reduced damping over a wide frequency range.

At low frequencies the solid curve in Fig. 4 resembles the damping results obtained by Quinlan *et al.*[18] for a tight-binding model because the *d*-wave gap dominates the damping. However, our results differ at higher frequencies, where nesting produces a linear ω form instead of the more complex variation that is determined by their use of the RPA series.

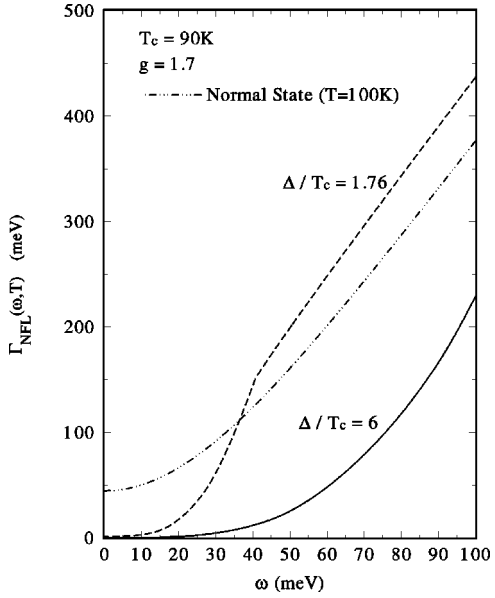

FIG. 4. The nested Fermi-liquid (NFL) damping shows the anomalous linear frequency variation—when $\omega \gg T$—by the dotted curve at 100 K. Using a superconducting transition temperature of $T_c=90$ K, the *d*-wave gap described in the text yields damping for weak coupling (dashed curve), while the solid curve exhibits the damping for the strong-coupling case $\Delta_{dm}=6T_c$.

The damping structure determines the microwave electrodynamics of YBCO as a function of frquency and temperature. Thus the present theoretical basis may provide guidance for higher frequency microwave applications.

III. ELECTROMAGNETIC RESPONSE FORMALISM

The theory of the electromagnetic response of superconductors was developed by Mattis and Bardeen[38] and by Abrikosov, Gorkov, and Khalatnikov.[39] The formalism was generalized to include anisotropic *p*-wave states by Klemm *et al.*[40] and by Hirschfeld *et al.*[41] In the context of the high-T_c cuprates, the theory of the electromagnetic response of *d*-wave superconductors was derived by Hirschfeld *et al.*[42] Therefore we will only sketch the formalism and refer the interested reader to the above references for details.

The current response of a superconductor to the vector potential of the incident electromagnetic wave with frequency ω is given by[43]

$$J(\vec{q},\omega)=R(\vec{q},\omega)\cdot\vec{A}(\vec{q},\omega), \tag{13}$$

with

$$R_{\alpha\beta}(\vec{q},\omega)=-e^2\left[\frac{n}{m}\delta_{\alpha\beta}+\langle\langle(J_\alpha J_\beta)\rangle\rangle(\vec{q},\omega)\right]. \tag{14}$$

The current-current correlation function is obtained from

$$\langle\langle(J_\alpha J_\beta)\rangle\rangle(\vec{q},i\nu_m)=\frac{1}{2}T\sum_{\vec{k},\omega_n} v_{\vec{k},\alpha}\mathrm{Tr}\left[\hat{G}\left(\vec{k}+\frac{\vec{q}}{2},i\omega_n\right)\times(v_{\vec{k},\beta}+\hat{Q}_\beta)\hat{G}\left(\vec{k}-\frac{\vec{q}}{2},i\omega_n+i\nu_m\right)\right] \tag{15}$$

by analytical continuation $i\nu_m\rightarrow\omega+i\delta$. Here $\hat{G}$ denotes the Nambu Green function for an anisotropic singlet superconductor. Treating isotropic impurity scattering in a $\hat{t}$-matrix approximation,[40] $\hat{G}$ can be written as

$$\hat{G}^{-1}(\vec{q},i\omega_n)=i\tilde{\omega}_n\hat{\tau}_0-\tilde{\epsilon}_k\hat{\tau}_3-\tilde{\Delta}_k\hat{\tau}_1. \tag{16}$$

For a *d*-wave superconductor,

$$i\tilde{\omega}_n=i\omega_n+\Gamma_{imp}\frac{g(i\omega_n)}{\cos^2\delta_N-\sin^2\delta_N g(i\omega_n)}, \tag{17}$$

$$\tilde{\epsilon}_k=\epsilon_k+\Gamma_{imp}\frac{1}{\cos^2\delta_N-\sin^2\delta_N g(i\omega_n)}, \tag{18}$$

and $\tilde{\Delta}_k=\Delta_k$. Here Γ_{imp} is the scattering rate, δ_N the corresponding phase shift, and

$$g(i\omega_n)=\frac{1}{\pi N_0}\sum_k\frac{i\tilde{\omega}_n}{(i\tilde{\omega}_n)^2-\tilde{\epsilon}_k^2-\tilde{\Delta}_k^2}. \tag{19}$$

The vertex corrections $\hat{Q}_\beta$ due to impurity scattering obey an integral equation, but our analysis simplifies because it can be shown that $\hat{Q}_\beta \equiv 0$ for a *d*-wave superconductor in the presence of isotropic impurity scattering. The momentum integrals are evaluated by the standard transformation

$$\sum_k f(\epsilon_k,\Delta_k) = N_0 \int_0^{2\pi} \frac{d\phi}{2\pi} \int_{-\infty}^{\infty} d\epsilon f(\epsilon,\Delta(\phi)). \tag{20}$$

Noting that the paramagnetic term $(n/m)\delta_{\alpha\beta}$ in Eq. (14) is cancelled by contributions to the momentum integral for the current-current correlation function from regions far away from the Fermi surface, one obtains in the local limit $\vec{q}\to 0$:

$$R_{\alpha\beta}(\vec{q},\omega) = R(\omega)\delta_{\alpha\beta}, \tag{21}$$

$$\begin{aligned} R(\omega) = \frac{1}{i\pi}\int_{-\omega/2}^{\infty} d\nu \left[\tanh\left(\frac{\nu+\omega}{2T}\right) - \tanh\left(\frac{\nu}{2T}\right)\right] \\ \times [M(\omega+\nu_+,\nu_-) - M(\omega+\nu_+,\nu_+)] \\ - \frac{2}{\pi}\int_{-\omega/2}^{\infty} d\nu \tanh\left(\frac{\omega+\nu}{2T}\right) \mathrm{Im}\, M(\omega+\nu_+,\nu_+), \end{aligned} \tag{22}$$

where $\nu_\pm = \nu \pm i\delta$, and

$$\begin{aligned} M(z_1,z_2) = \frac{1}{2}\int_0^{\pi/2} d\phi \left[1 + \frac{\tilde{z}_1\tilde{z}_2 + \Delta_m \cos^2(2\phi)}{w(\tilde{z}_1)w(\tilde{z}_2)}\right] \\ \times \left[\frac{1}{w(\tilde{z}_1)+w(\tilde{z}_2)+\rho(z_1,z_2)} \right. \\ \left. + \frac{1}{w(\tilde{z}_1)+w(\tilde{z}_2)-\rho(z_1,z_2)}\right], \end{aligned} \tag{23}$$

$$w(z) = \sqrt{\Delta_m^2 \cos^2(2\phi) - z^2}, \tag{24}$$

$$\begin{aligned} \rho(z_1,z_2) = \Gamma_{imp}\frac{\cos\delta_N}{\sin\delta_N}\left[\frac{1}{\cos^2\delta_N - \sin^2\delta_N g(z_1)} \right. \\ \left. - \frac{1}{\cos^2\delta_N - \sin^2\delta_N g(z_2)}\right], \end{aligned} \tag{25}$$

and

$$\tilde{z}(z) = z + \Gamma_{imp}\frac{g(z)}{\cos^2\delta_N - \sin^2\delta_N g(z)} - i\Gamma_{NFL}(z,T), \tag{26}$$

where $g(z)$ follows from analytic continuation and a momentum integration of the Green's function in Eq. (19).

Defining the impurity concentration n_{imp} and damping Γ_{imp}, the component of the *t* matrix in the Born approximation is

$$-n_{imp}t_0(z) = i\Gamma_{imp} g(z), \tag{27}$$

whereas the strong scattering (unitary) limit gives

$$-n_{imp}t(z) = i\Gamma_{imp}\frac{1}{g(z)}. \tag{28}$$

Here $g(z)$ has to be calculated self-consistently from Eq. (19) and

$$g(z) = -i\int_0^{2\pi}\frac{d\phi}{2\pi}\frac{\tilde{z}}{\sqrt{\Delta_m^2\cos^2(2\phi)-\tilde{z}^2}}. \tag{29}$$

We presume that the damping $\Gamma_{NFL}(z,T)$ is independent of momentum along the nested regions, and thus does not depend on the angle ϕ. This step simplifies the integration in the above equations, but leaves out damping from non-nested regions, which may resemble the Fermi-liquid form. Our analysis also neglects electron-phonon contributions, and chooses the dilute impurity limit. The curves in the present paper are calculated in the limit of small Γ_{imp}, in order to emphasize the influence of the frequency and temperature variation of the nested electron collision damping Γ_{NFL} on the microwave response of high-T_c superconductors.

IV. MICROWAVE PROPERTIES

A. Surface resistance below T_c

The surface resistance $R_s(\omega,T)$ is given in terms of the response function $R(\omega,T)$:

$$R_s(\omega,T) = Z_0\frac{\omega\lambda_L}{c}\mathrm{Re}\frac{1}{\sqrt{-R(\omega,T)}}, \tag{30}$$

where $Z_0 = 377\ \Omega$ is the surface impedance of vacuum and the London penetration depth is $\lambda_L \approx 1640$ Å for the plasma frequency of $\omega_{pl} = 1.2$ eV that we use for YBCO.

In the limit of negligible impurity scattering, the electron collision damping Γ_{NFL} from Eqs. (4), (10), and (12) is inserted into Eqs. (22)–(30), and then a numerical integration yields the surface resistance curves shown in Fig. 5. The standard weak-coupling *d*-wave gap yields the dashed curve which is far above experiment for T near T_c. The sudden drop in R_s just below $T_c = 90$ K in the Hardy group data,[3] is explained by the strong-coupling solid curve for $\Delta_{dm} = 6T_c$ in Fig. 5, because the larger gap significantly decreases available scattering states. At intermediate T the surface resistance for the strong-coupling case is somewhat below the data, although the logarithmic scale exagerrates this discrepancy. Impurity scattering or another parameter set may modify the flat region of the microwave resistance data in the range 30–80 K, but it should be noted that recent experiments on untwinned YBCO crystals by Zhang *et al.*[44] yield a maximum in R_s in the intermediate temperature range, and a steep falloff in R_s below 10 K which agree qualitatively with our calculated solid curve.

Tight-binding energy-band model calculations by Hirschfeld *et al.*[42] also yield a good description of the microwave R_s as a function of T (for $T<T_c$), and their treatment of impurity scattering agrees with experimental trends. Thus a systematic analysis of the microwave response at various T and ω values is required to distinguish our nesting results from alternate approaches.

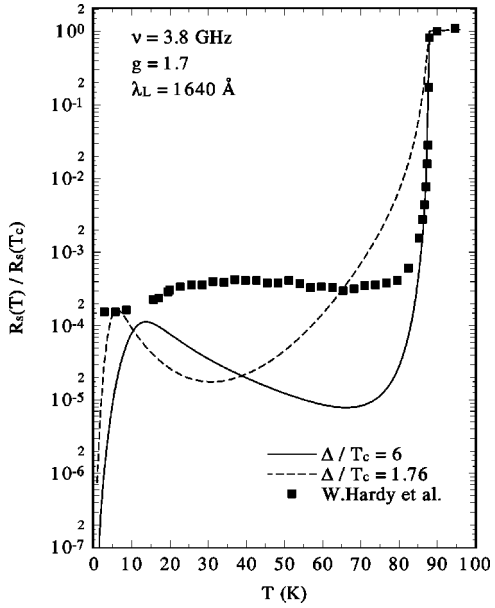

FIG. 5. The calculated microwave surface resistance for a superconductor with a *d*-wave energy gap and NFL damping exhibits the steep decline just below T_c in the case of the solid curve for the strong-coupling gap $\Delta_{dm}=6T_c$. The broad bump near 20 K is seen in more recent experiments on untwinned YBCO crystals. The experimental squares for YBCO are from Ref. 3. The dashed curve shows the T dependence of R_s for the weak-coupling gap case with $\Delta_{dm}=1.76T_c$.

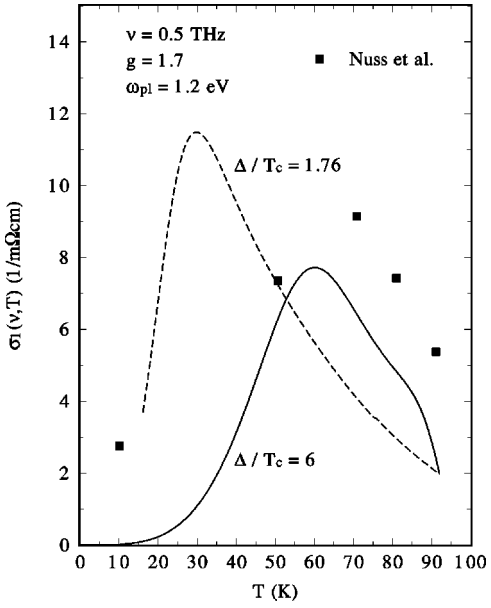

FIG. 6. A peak in the conductivity of YBCO in the superconducting state is shown as a function of temperature by the data squares from Ref. 7 at a frequency $\nu=0.5$ THz. The NFL damping with a *d*-wave energy gap produces the peak structure shown by the dashed curve for a weak coupling, and the solid curve for the strong-coupling case $\Delta_{dm}=6T_c$. Such conductivity peaks are sensitive to impurity scattering.

In a realistic material, segments of the Fermi surface that do not satisfy the nesting condition would add a separate scattering rate, e.g., a Fermi-liquid form, or perhaps some electron-phonon contribution. However, inclusion of another damping rate would introduce additional parameters without constraints or a well-defined justification.

B. Infrared conductivity

The optical conductivity $\sigma(\omega,T)$ of cuprates at room temperature falls off as $\sigma_1\approx 1/\omega$ rather than the standard Drude behavior $\sigma_1\propto 1/\omega^2$. This anomaly characterizes all the high-T_c materials, and suggests a damping that is proportional to ω over a wide frequency range (up to 1 eV). A microscopic theory of the optical conductivity in the long-wavelength regime incorporates self-energy and vertex corrections that satisfy the Ward identity,[45] and this NFL conductivity fits various cuprate experiments for $T>T_c$.[1]

The above formalism yields the conductivity for a *d*-wave superconductor

$$\sigma(\omega,T)=-\frac{\omega_{pl}^2 R(\omega,T)}{i\omega}, \tag{31}$$

which can be computed by a numerical integration of Eqs. (22)–(30). The resulting temperature variation of the conductivity is shown in Fig. 6 in comparison to the experimental points of Nuss *et al.*[7] for a relatively large microwave frequency $\nu=0.5$ THz. The weak-coupling *d*-wave dashed curve shows a peak at low T, while the strong-coupling *d* wave with $\Delta_{dm}=6T_c$ yields the solid curve and a peak closer to the experimental points. These calculations use the same Coulomb coupling $UN(0)=1.7$ as in the surface resistance analysis, and a renormalized plasma frequency of 1.2 eV that is compatible with previous analysis[45] of the YBCO reflectivity.

The frequency variation of the computed conductivity is shown in Fig. 7 for two temperatures. Above T_c the $1/\omega$ dependence of σ_1 is shown by the solid curve for $T=95$ K, where impurity scattering was not included even though it may improve agreement at low ω. The unusual non-Drude

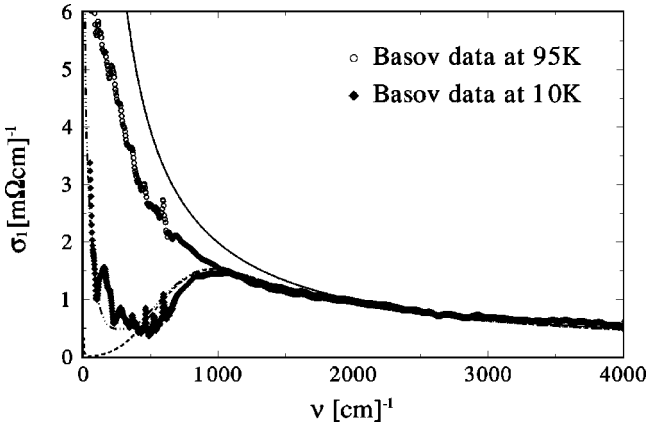

FIG. 7. Microwave conductivity data (circles) as a function of frequency show the anomalous normal-state behavior $\sigma_1\sim\omega^{-1}$ (that is a hallmark for all high-T_c cuprates). The solid curve is calculated with NFL damping $g=0.74$ at 100 K. For a *d*-wave superconductor with $T_c=90$ K, the strong-coupling state with $\Delta_{dm}=4.2T_c$ gives the dashed curve at a temperature $T=10$ K, which resembles the data (diamonds) measured by Basov *et al.* in Ref. 47 on YBCO. The dot-dash curve includes impurity scattering with $\Gamma_{imp}=0.2$ meV and $\delta N=0.4\pi$ in addition to the NFL damping.

behavior $\sigma \approx \omega^{-1}$ extends up to 1 eV (roughly 8000 cm^{-1}) in all high-T_c cuprates. This mysterious behavior arises from a linear ω variation of the damping and therefore provides a primary distinction for theories. Our analysis yields the strange conductivity directly as a consequence of electron collisions on a nested path.

Tight-binding model computations by Quinlan *et al.*[18] show a larger drop in the conductivity with increasing ω, which may be due to a more complex damping which depends on the RPA series. A standard Fermi liquid has a damping proportional to ω^2, and this would imply a conductivity that drops more rapidly than the cuprate data at high ω.

Electron-phonon damping should be roughly independent of ω in the range above the Debye cutoff,[6] but instead should show a large T dependence. These characteristic phonon properties are apparent in the optical spectra of lead,[1] although they are not evident in the conductivity data for YBCO in Fig. 7

The high-frequency conductivity is also sensitive to phenomenological models that represent a Boson-mediated damping. For example, the Boson spectrum cutoff used by Carbotte's group[46,48] yields a nearly constant σ when ω is larger than the cutoff, as one may expect from the original formal Holstein analysis.[6]

In the superconducting state the dashed curve shows the computed NFL conductivity, which is reduced by a *d*-wave gap, in qualitative agreement with the infrared spectra of YBCO measured by Basov *et al.*[47] in Fig. 7. The dot-dash curve demonstrates the influence of impurity scattering which raises the conductivity in the superconducting state at very low frequency.

These superconducting state data are also compatible with computations by Quinlan *et al.*,[18] and others, in part because the *d*-wave gap dominates the response at very low ω. The Carbotte group[48] also achieved a good fit in the superconducting regime with their Boson spectrum, and furthermore found a good description of the impurity influence on the low-frequency conductivity.

C. Optical reflectivity

The infrared reflectivity $\mathcal{R}(\omega,T)$ is defined in terms of the dielectric function ε as

$$\mathcal{R}(\omega,T)=\left|\frac{\sqrt{\varepsilon(\omega,T)}-1}{\sqrt{\varepsilon(\omega,T)}+1}\right|^2, \tag{32}$$

where

$$\varepsilon(\omega,T)=\varepsilon_\infty-\frac{\omega_{pl}^2}{\omega^2}K(\omega,T), \tag{33}$$

ω_{pl} is the plasma frequency, and ε_∞ is the dielectric constant of the background.

The computed NFL reflectivity is shown in Fig. 8 by the solid curve alongside the 100 K data on untwinned YBCO crystals obtained by Schlesinger *et al.*;[49] note that this normal-state curve determines the plasma frequency of $\omega_{pl}/\sqrt{\varepsilon_\infty}=1.2$ eV and the Coulomb coupling $UN(0)=0.74$ from a fit to the data (triangles) at 100 K. The superconducting curve at 33 K follows for the same coupling and plasma frequency, and thus only the *d*-wave gap amplitude remains as an independent parameter.

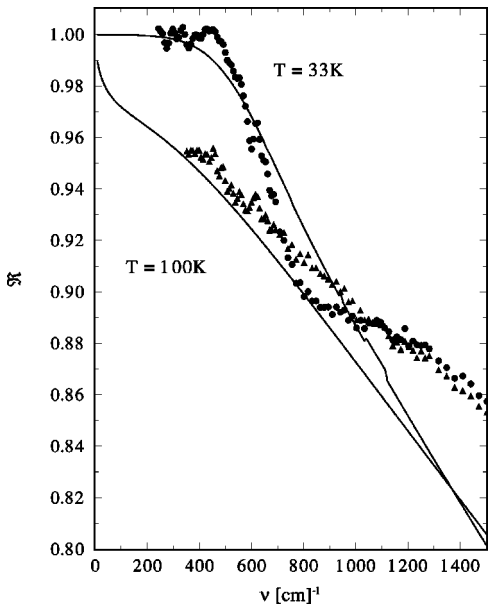

FIG. 8. Infrared data for YBCO from Ref. 49 show the anomalous reflectivity decline as a function of frequency for the normal state by triangles, and the superconducting state data by open circles. The dotted curve is the NFL reflectivity computed at 100 K. The *d*-wave energy gap yields the upper curve, with the strong coupling case $\Delta_{dm}=3T_c$ and $T_c=92$ K. The plasma frequency is $\omega_{pl}/\sqrt{\epsilon_0}=1.2$ eV and the Coulomb repulsion is $UN(0)=0.74$.

The independent reflectivity data of Basov *et al.*[47] on YBCO and the 124 compound also show the low-frequency threshold structure in the superconducting state, although a strong anisotropy along the *a* and *b* axes of the crystal may be caused by effective mass differences.

Several years ago, reflectivity data on cuprates were interpreted as evidence for the absence of an energy gap by some authors. The present work shows that the single-crystal $R(\omega)$ data of Schlesinger *et al.*[49] and others is compatible with a strong-coupling *d*-wave gap.

D. Penetration depth

The penetration depth $\lambda(\omega,T)$ probes the superfluid density n_s, which is determined by the density of states in the gap region. Thermal excitation of quasiparticles depends on the symmetry as well as the magnitude of the energy gap in the superconducting state, and these fundamental features determine the temperature variation of λ.

The classic BCS model of an isotropic energy gap Δ_s gives the behavior

$$\Delta\lambda_{BCS}=\lambda(T)/\lambda(0)-1=3.3\sqrt{T/T_c}\,\exp[-1.76T_c/T] \tag{34}$$

and this form is essentially verified by measurements by Anlage *et al.*[51] on Nb and also on the electron-doped NCCO cuprate. The NCCO case is very interesting since the BCS behavior of the penetration depth holds despite strong inelastic Fermi-liquid collisions and substantial impurity scattering in these crystal samples.

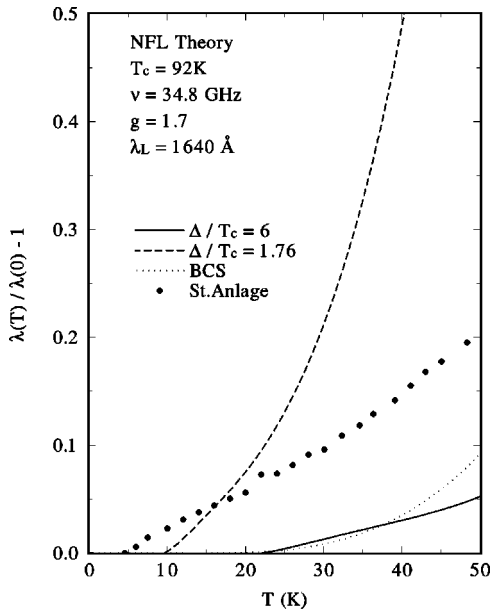

FIG. 9. Penetration depth data points from Ref. 51 for the YBCO superconducting state contrast with the standard BCS model shown by the dotted curve. The *d*-wave gap, combined with the nested collision damping analysis, yields the dashed curve for the weak-coupling case, while the solid curve shows the NFL penetration depth for the strong-coupling case of $\Delta_{\max}=6T_c$. The data points to a strong-coupling value, in the range $\Delta_{dm}\sim 4T_c$, which would agree with the conductivity analysis.

Gros *et al.*[35] derived penetration depth formulas for unconventional pairing such as *p*-wave and *d*-wave states, and they showed that various power laws for the penetration depth $\lambda \propto T^n$ can occur, where the exponent n depends on the type of nodes and the orientation of the applied field. The linear T variation of λ for a d-wave state is particularly relevant to high-T_c cuprates even though the original Gros group analysis was aimed at the heavy-fermion superconductors whose T_c values are very low (~ 1 K).

Annett *et al.*[50] showed that unconventional singlet pairs, such as the *d*-wave pairs, in a two-dimensional system will generally yield a linear T variation of the penetration depth. Recent microwave experiments on high-quality crystals of YBCO show such a linear T variation, as illustrated by the Anlage[51] data in Fig. 9. By contrast, the BCS dotted curve from Eq. (34) shows the activated temperature form caused by a *s*-wave gap which is much lower than experiment. Microwave studies[52] of Bi2212 crystals also yield a linear T variation of λ up to 40 K.

Our microscopic theory considers the standard relation for the penetration depth

$$\lambda(\omega,T) = -\lambda_L \mathrm{Im}\frac{1}{\sqrt{-K(\omega,T)}}, \tag{35}$$

where $\lambda_L = c/\omega_{pl}$ is the London penetration depth. The calculated penetration depth for a *d*-wave energy gap in the NFL approximation is shown in Fig. 9 by the dashed curve for weak coupling and by the solid curve for the strong-coupling case. Since the experimental points of Anlage *et al.*[51] fall in between the weak-coupling and very strong-coupling curves, they provide support for a large gap value (near $\Delta_{dm}\approx 4T_c$) which would be compatible with the conductivity analysis of the YBCO cuprate.

Earlier penetration depth on films and some other samples seemed to show a T^2 variation in cuprates, which would appear to contradict both the BCS and *d*-wave scenarios.[50] However, controlled doping of YBCO crystal with Zn and Ni by Hardy's group[44] demostrated a crossover from the intrinsic linear T variation in the untwinned crystal to a quadratic form in impure cases. Theoretical proposals for the crossover in temperature variation include the role of scattering by impurities[42] and the nonlocal electrodynamics that are essential in the *d*-wave case because the associated coherence length must be treated with care.[53]

V. CONCLUSIONS

Our analysis of the microwave electrodynamics indicates a metallic character of the electrons (or holes) with a plasma frequency comparable to ordinary metals. We explain various unconventional features of the microwave response of superconducting cuprates within the NFL theory framework of electrons scattering on nested paths with a Coulomb coupling that is comparable to the bandwidth.

The dramatic drop of the microwave surface resistance in the superconducting state of YBCO and BSCO cuprates is attributed to the opening of an energy gap with *d*-wave symmetry which depletes available scattering states for the target as well as the scattering electron. However, the calculated frequency variation as well as the temperature variation of the NFL damping in the superconducting state are compatible with the measured high-T_c cuprate conductivity only if the energy gap is quite large. Although many other groups have properly identified the source of the microwave decrease with a surprising damping reduction, our analysis yields conductivity features at higher frequencies which differ from the results of tight-binding calculations and some Boson spectral models.

Our theoretical basis for the damping involves a peculiar scaling of the spin susceptibility—as a function of ω/T—which has been observed by neutron scattering in cuprates. The scaling yields the strange non-Drude form of the conductivity $\sigma \approx \omega^{-1}$ which persists to 1 eV. At low ω the *d*-wave energy gap dominates the spectral response, so our results for this region are similar in many respects to previous calculations based on tight-binding models or Boson-style spectra. In view of many competing explanations for the low-frequency conductivity, further systematic analysis of the frequency and T variation in the superconducting state is warranted.

Theoretical proposals for a large gap ratio in cuprates generally make a connection to the strong electron damping that is a key feature of the cuprates. Lee and Read[54] originally noted that inelastic damping would reduce the superconducting temperature. Calculations for tight-binding energy-band models[55,56] find that exchange of spin fluctuations can generate a large gap ratio by using the RPA enhancement of the spin susceptibility. Self-energy contributions in a square nesting model[57] yield a temperature variation of the spin susceptibility which produces a large gap ratio in the leading order *d*-wave pairing theory.

Both the magnitude of the NFL collision damping and the

large superconducting gap ratio require a theoretical analysis of higher-order self-energy and vertex corrections on a consistent basis. Recently Aeppli *et al.*[29] discovered a susceptibility which diverges as $T^{-\alpha}$ when T is lowered toward the superconducting transition in $La_{1.86}Sr_{0.24}CuO_4$. This low-frequency anomaly stimulated a theory[28] for a nested surface which produces a singular spin susceptibility, where the T variation exponent α is proportional to the Coulomb repulsion. The latter analysis sums leading logarithmically divergent vertex corrections to all orders in U using the Parquet method, and demonstrates the failure of the RPA in the case of nesting. Remarkably, a similar divergence in the low-frequency susceptibility was observed by neutron scattering near the nesting vector in chromium many years ago.[58] Recent neutron data[59] on the itinerant antiferromagnet V_2O_3 discovered a spin susceptibility that diverges with a power-law exponent that is almost identical to the situation for the high-T_c LSCO cuprate. Clearly the Parquet series of graphs should be examined in future extensions of the present analysis of the microwave properties.

Experiments with cuprates under applied pressure should provide interesting tests of the *d*-wave structure as well as the present theoretical proposals. Pressure increases T_c by as much as 50 K in some mercury based cuprates, so the corresponding enlargement of the energy gap should produce rather significant modifications in the microwave response of these high-temperature superconductors.

ACKNOWLEDGMENTS

It is a pleasure to thank D. Djajaputra, M.H. Cohen, W.A. Little, S. Tewari, and A. Virosztek for stimulating discussions. We are indebted to S. Anlage, D. Basov, W. Hardy, and Z. Schlesinger for sending us experimental data. Our research was supported by DOE Grant No. DEFG05-84ER45113. C.T.R. gratefully acknowledges a grant from the Deutsche Forschungsgemeinschaft via the Graduiertenkolleg ''Physik nanostrukturierter Festkorperphysik.''

[1] A review of cuprate anomalies and theory prospects is in J. Ruvalds, Supercond. Sci. Technol. **9**, 905 (1996).
[2] A. Virosztek and J. Ruvalds, Phys. Rev. B **42**, 4064 (1990).
[3] D.A. Bonn, P. Dosanjh, R. Liang, and W.N. Hardy, Phys. Rev. Lett. **68**, 2390 (1992).
[4] G. Rickayzen, *Theory of Superconductivity* (Interscience, New York, 1965). The influence of phonon damping is derived in Phys. Rev. **156**, 470 (1967).
[5] H.J. Fink, Phys. Rev. B **58**, 9415 (1998).
[6] R.F. Wallis and M. Balkanski, ''Many-body aspects of solid state spectroscopy'' (North-Holland, New York, 1986).
[7] M.C. Nuss, P.B. Littlewood, S. Schmitt-Rink, E. Abrahams, and A.E. Ruckenstein, Phys. Rev. Lett. **66**, 3305 (1991).
[8] C.M. Varma, P.M. Mankiewitz, M.L. O'Malley, E.H. Westerwick, and P.B. Littlewood, Phys. Rev. Lett. **63**, 1996 (1989).
[9] C.T. Rieck, W.A. Little, J. Ruvalds, and A. Virosztek, Phys. Rev. B **51**, 3772 (1995).
[10] S. Hansen, G. Muller, C.T. Rieck, and K. Scharnberg, Phys. Rev. B **56**, 6237 (1997).
[11] M. Ogata and P.W. Anderson, Phys. Rev. Lett. **70**, 3087 (1993).
[12] J. Voit, Rep. Prog. Phys. **57**, 977 (1994).
[13] E.J. Nicol and J.P. Carbotte, Phys. Rev. B **44**, 7741 (1991).
[14] Th. Dahm, S. Wermbter, and L. Tewordt, Physica C **190**, 537 (1992).
[15] S. Quinlan, D.J. Scalapino, and N. Bulut, Phys. Rev. B **49**, 1470 (1994).
[16] P.B. Littlewood and C.M. Varma, J. Appl. Phys. **69**, 4979 (1991).
[17] B.W. Statt and A. Griffin, Phys. Rev. B **46**, 3199 (1992).
[18] S.M. Quinlan, P.J. Hirschfeld, and D.J. Scalapino, Phys. Rev. B **53**, 8575 (1996).
[19] D.J. Van Harlingen, Rev. Mod. Phys. **67**, 515 (1995).
[20] D.M. King *et al.*, Phys. Rev. Lett. **70**, 3159 (1993).
[21] S.M. Anlage *et al.*, Phys. Rev. B **50**, 523 (1994).
[22] N.F. Berk and J.R. Schrieffer, Phys. Rev. Lett. **17**, 433 (1966).
[23] A.W. Overhauser, Phys. Rev. **128**, 1437 (1962).
[24] W. Kohn and J.M. Luttinger, Phys. Rev. Lett. **15**, 524 (1965).
[25] D.J. Scalapino, Phys. Rep. **250**, 329 (1995).
[26] J.R. Schrieffer, J. Low Temp. Phys. **99**, 397 (1995).
[27] N.E. Bickers, Int. J. Mod. Phys. B **5**, 253 (1991).
[28] D. Djajaputra and J. Ruvalds, Solid State Commun. **111**, 199 (1999).
[29] G. Aeppli *et al.*, Science **278**, 1432 (1997).
[30] J. Ruvalds, C.T. Rieck, S. Tewari, J. Thoma, and A. Virosztek, Phys. Rev. B **51**, 3797 (1995).
[31] D.S. Dessau *et al.*, Phys. Rev. Lett. **71**, 2781 (1993).
[32] J. Rossat-Mignod *et al.*, Physica B **169**, 58 (1991).
[33] A. Virosztek and J. Ruvalds, Phys. Rev. B **59**, 1324 (1999).
[34] A.T. Zheleznyak, V.M. Yakovenko, and I.E. Dzyaloshinski, Phys. Rev. B **55**, 3200 (1997).
[35] F. Gros *et al.*, Z. Phys. B **64**, 175 (1986).
[36] T.E. Mason, A. Schroder, G. Aeppli, H.A. Mook, and S.M. Hayden, Phys. Rev. Lett. **77**, 1604 (1996).
[37] T.E. Mason, G. Aeppli, S.M. Hayden, A.P. Ramirez, and H.A. Mook, Phys. Rev. Lett. **71**, 919 (1993).
[38] D.C. Mattis and J. Bardeen, Phys. Rev. **111**, 412 (1958).
[39] A.A. Abrikosov, L.P. Gor'kov, and I.M. Khalatnikov, Zh. Éksp. Teor. Fiz. **5**, 265 (1958) [Sov. Phys. JETP **8**, 182 (1959)]; A.A. Abrikosov and L.P. Gor'kov, *ibid.* **39**, 1781 (1960) [**12**, 1243 (1961)].
[40] R.A. Klemm, K. Scharnberg, D. Walker, and C.T. Rieck, Z. Phys. B **72**, 139 (1988).
[41] P.J. Hirschfeld, P. Wölfle, J.A. Sauls, D. Einzel, and W.O. Puttika, Phys. Rev. B **40**, 6695 (1989).
[42] P.J. Hirschfeld, W.O. Putikka, and D.J. Scalapino, Phys. Rev. B **71**, 3705 (1993); Phys. Rev. B **50**, 10 250 (1994).
[43] J.R. Schrieffer, *Theory of Superconductivity* (Addison-Wesley, Redwood City, 1964).
[44] K. Zhang *et al.*, Phys. Rev. Lett. **73**, 2484 (1994).
[45] J. Ruvalds and A. Virosztek, Phys. Rev. B **43**, 5498 (1991).
[46] E. Schachinger and J.P. Carbotte, Phys. Rev. B **57**, 7970 (1998).
[47] D.N. Basov *et al.*, Phys. Rev. Lett. **74**, 598 (1995).
[48] J.P. Carbotte, C. Jiang, D.N. Basov, and T. Timusk, Phys. Rev. B **51**, 11 798 (1995).

[49] Z. Schlesinger *et al.*, Phys. Rev. Lett. **65**, 801 (1990).
[50] J. Annett, N. Goldenfeld, and S.R. Renn, Phys. Rev. B **43**, 2778 (1991).
[51] S.M. Anlage *et al.*, Phys. Rev. B **50**, 523 (1994).
[52] S.F. Lee *et al.*, Phys. Rev. Lett. **77**, 735 (1996).
[53] I. Kosztin and A. J. Leggett, Phys. Rev. Lett. **79**, 135 (1997).
[54] P.A. Lee and N. Read, Phys. Rev. Lett. **58**, 2691 (1987).
[55] C.H. Pao and N.E. Bickers, Phys. Rev. Lett. **72**, 1870 (1994).
[56] P. Monthoux and D.J. Scalapino, Phys. Rev. Lett. **72**, 1874 (1994).
[57] D. Djajaputra and J. Ruvalds, Phys. Rev. B **55**, 14 148 (1997).
[58] B.H. Grier, Jr., G. Shirane, and S.A. Werner, Phys. Rev. B **31**, 2892 (1985).
[59] Wei Bao, C. Broholm, J.M. Honig, P. Metcalf, and S.F. Trevino, Phys. Rev. B **54**, R3726 (1996); **58**, 12 727 (1998).